

Accepted Manuscript

Systematic diversification of benzylidene heterocycles yields novel inhibitor scaffolds selective for Dyrk1A, Clk1 and CK2

Marica Mariano, Rolf W. Hartmann, Matthias Engel



PII: S0223-5234(16)30087-3

DOI: [10.1016/j.ejmech.2016.02.017](https://doi.org/10.1016/j.ejmech.2016.02.017)

Reference: EJMECH 8368

To appear in: *European Journal of Medicinal Chemistry*

Received Date: 14 December 2015

Revised Date: 4 February 2016

Accepted Date: 5 February 2016

Please cite this article as: M. Mariano, R.W. Hartmann, M. Engel, Systematic diversification of benzylidene heterocycles yields novel inhibitor scaffolds selective for Dyrk1A, Clk1 and CK2, *European Journal of Medicinal Chemistry* (2016), doi: 10.1016/j.ejmech.2016.02.017.

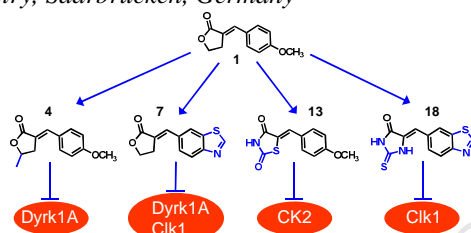
This is a PDF file of an unedited manuscript that has been accepted for publication. As a service to our customers we are providing this early version of the manuscript. The manuscript will undergo copyediting, typesetting, and review of the resulting proof before it is published in its final form. Please note that during the production process errors may be discovered which could affect the content, and all legal disclaimers that apply to the journal pertain.

Graphical Abstract

Systematic diversification of benzylidene heterocycles yields novel inhibitor scaffolds selective for Dyrk1A, Clk1 and CK2

Leave this area blank for abstract info.

Marica Mariano, Rolf W. Hartmann, Matthias Engel
Pharmaceutical and Medicinal Chemistry, Saarbrücken, Germany





Systematic diversification of benzylidene heterocycles yields novel inhibitor scaffolds selective for Dyrk1A, Clk1 and CK2

Marica Mariano^a, Rolf W. Hartmann^{a,b} and Matthias Engel^{a,*}

^a Department of Pharmaceutical and Medicinal Chemistry, Saarland University, Saarbrücken, Germany.

^b Helmholtz Institute for Pharmaceutical Research Saarland (HIPS), Campus C2-3, D 66123 Saarbrücken, Germany

ARTICLE INFO

Article history:

Received

Received in revised form

Accepted

Available online

Keywords:

Dyrk1A

PI3 kinase

Alzheimer

glioma

multi-targeted inhibitor

ABSTRACT

The dual-specificity tyrosine-regulated kinase 1A (Dyrk1A) has gathered much interest as a pharmacological target in Alzheimer's disease (AD), but it plays a role in malignant brain tumors as well. As both diseases are multi-factorial, further protein kinases, such as Clk1 and CK2, were proposed to contribute to the pathogenesis. We designed a new class of α -benzylidene- γ -butyrolactone inhibitors that showed low micromolar potencies against Dyrk1A and/or Clk1 and a good selectivity profile among the most frequently reported off-target kinases. A systematic replacement of the heterocyclic moiety gave access to further inhibitor classes with interesting selectivity profiles, demonstrating that the benzylidene heterocycles provide a versatile tool box for developing inhibitors of the CMGC kinase family members Dyr1A/1B, Clk1/4 and CK2. Efficacy for the inhibition of Dyrk1A-mediated tau phosphorylation was demonstrated in a cell-based assay. Multi-targeted but not non-specific kinase inhibitors were also obtained, that co-inhibited the lipid kinases PI3K α/γ . These compounds were shown to inhibit the proliferation of U87MG cells in the low micromolar range. Based on the molecular properties, the inhibitors described here hold promise for CNS activity.

2009 Elsevier Ltd. All rights reserved.

* Corresponding author. E-mail: ma.engel@mx.uni-saarland.de; phone: +4968130270312.

1. Introduction

The dual-specificity tyrosine-regulated kinases (Dyrk) and CDC2-like kinases (Clk) both belong to the CMGC branch of the kinome and share the ability to phosphorylate tyrosine as well as serine/threonine residues; however, only the activating autophosphorylation occurs actually at tyrosine.

The Dyrk1A isoform is expressed ubiquitously while the most closely related homolog, Dyrk1B, is mainly found in testes and muscle tissue [1]. In the last decade, Dyrk1A, but not Dyrk1B, received much attention due to its implication in the development of Down Syndrome-related and sporadic Alzheimer's disease (AD) [2,3], where it promotes neurodegeneration by hyperphosphorylating the microtubule-associated protein tau [4]. Furthermore, Dyrk1A was also shown to phosphorylate amyloid precursor protein (APP) and presenilin-1, a key component of the γ -secretase complex, thereby accelerating the formation of neurotoxic A β peptides [5].

Recently, Dyrk1A was also proposed as a new target in glioblastoma [6]. Glioma are among the most malignant types of solid tumors and survival rates for patients are still very poor: less than 5% of patients survive for 5 years after having been diagnosed with glioblastoma multiforme, the most aggressive subtype [7]. Hence, more effective therapeutic agents are urgently needed. Of note, Dyrk1A was reported to act as an enhancer of receptor tyrosine kinase signaling; known examples include FGFR [8] and EGFR [6,9]. Pozo and coworkers found Dyrk1A to be strongly overexpressed in glioblastoma, paralleling EGFR expression [6]. Dyrk1A prevents endocytosis-mediated degradation of EGFR by a mechanism that requires phosphorylation of the EGFR signaling modulator Sprouty2 [9]. Moreover, Dyrk1A-catalyzed phosphorylation of FOXO (also called FKHR) was shown to promote nuclear exclusion, thus maintaining cell cycle progression and suppressing the activation of pro-apoptotic genes [10,11]. Compared with healthy tissue, the mRNA of Dyrk1A, but not of the homologous kinases Dyrk1B or Dyrk2, was strongly overexpressed in glioblastoma, medulloblastoma, astrocytoma and oligodendroglioma (analyzed using the Oncomine portal, www.oncomine.org) [12,13]. This suggests that Dyrk1A could be an interesting anti-cancer target in EGFR-overexpressing tumors.

The Clk1 and -4 isoforms do not only share a strong structural homology with the Dyrk family but also some physiological functions: Both are involved in the regulation of alternative mRNA splicing through the phosphorylation of serine-arginine-rich (SR) proteins, including AF2/ASF, SC35 and SRp55 [14–18].

SR proteins mostly promote the inclusion of exons *via* binding to exonic splicing enhancers, and their activity is mainly regulated by multiple phosphorylations [19,20]. Upon dysregulation of the kinase activities in the case of Alzheimer's disease, the alternative splicing of tau is influenced, which results in a pathogenic imbalance between 3R-tau and 4R-tau isoforms through skipping of exon 10 [17]. Thus, co-inhibition of Dyrk and Clk kinases might efficiently correct the tau splicing isoform imbalance. Indeed, we could show that dual inhibitors of Dyrk1A and Clk1 are more efficient pre-mRNA splicing modulators than selective Dyrk1A or Clk1 inhibitors [21]. Furthermore, Leucettine L41, a dual Dyrk1A/Clk1 inhibitor [22] was recently reported to prevent memory impairments and neurotoxicity induced by oligomeric A β_{25-35} peptide administration in mice [23].

However, whether the benefit of such multi-targeted approaches outweighs the potential accumulation of side effects related to target inhibitions, will only be seen in long term *in*

in vivo studies. Therefore, a selective inhibitor of Dyrk1A is a primary goal of drug development efforts, in particular with respect to Down Syndrome-related neurodegeneration, for which the overexpression of Dyrk1A is a main cause [24].

Rather selective Dyrk1A inhibitors have been described previously, such as harmine, INDY, KH-CB19, Leucettines and pyridinylthiophenes [25–29], however, they still inhibited Clk1/4 with equal potency. Recently, Falke *et al.* [30] reported some 10-iodo-11*H*-indolo[3,2-*c*]quinoline-6-carboxylic acid derivatives as highly selective inhibitors of Dyrk1A, but the carboxylic acid function may impair CNS penetration [31].

From a medicinal chemistry point of view, it is advantageous that Dyrk1A can potentially be inhibited by very small molecules with molecular weights below 300 g/mol [25,26], suggesting that the binding site can adapt to small ligands. This property contributes to the attractiveness of Dyrk1A as a target for CNS diseases, because as a rule of thumb, the smaller the inhibitor, the higher are the chances to pass the blood brain barrier [31].

In the following, we describe the development of small benzylidene derivatives, which cover a broad range of selectivity and potency profiles, depending on the combined heterocycles.

2. Results and discussion

2.1. Design strategy and synthesis

Two of the most important factors that determine the CNS permeability of small molecules are the molecular mass, which showed a median of 305 Da in a thorough analysis of CNS drugs, and the number of H-bond donors, which should be ≤ 1 [31]. Therefore, our design of new Dyrk1A inhibitors was based on previously published inhibitors that fulfilled the following criteria: i) low mass, ii) no requirement for an H-bond donor contacting the hinge region, and iii) good potency in cellular systems. One of the most compact but yet potent and orally available inhibitor of Dyrk1A is the β -carboline alkaloid harmine (Figure 1). *In vitro* studies showed good activity against Dyrk1A, particularly in cells, and a slight selectivity toward other members of the Dyrk family. However, it also exerts several adverse CNS effects due to its potent monoaminoxidase-A inhibition [32]. The benzothiazole TG003 is a synthetic inhibitor of Dyrk1A which was identified in a high-throughput screening [26]. This compound is able to block the negative regulatory activity of Dyrk1A in the NFAT pathway. Unfortunately, its potency is not sufficient for *in vivo* applications (cell-free IC₅₀ for Dyrk1A: 0.8 μ M) [21]. Another rather small compound with inhibitory activity against Dyrks and Clk1 is leucettamine B, which was isolated from a marine sponge [22].

A superimposition of harmine, INDY (the 5-hydroxy derivative of TG003) and Leucettine L41 (a synthetic derivative of Leucettamine B [22]) as bound to Dyrk1A in published cocrystal structures revealed some common pharmacophoric features, which were used as starting points for the design of new Dyrk1A inhibitors (Figure 2). Obviously, two H-bond acceptor (HBA) functions at the molecule ends and an aromatic system connected to one HBA were sufficient for strong binding affinity to the ATP binding cleft of Dyrk1A. The smallest possible linker to connect two suitable moieties, which preserved the planar overall geometry, was a methine bridge. This was already present in the Leucettamine derivatives (Figure 1), in which the 2-aminoimidazolone carbonyl oxygen was functioning as HBA for Lys188. Employing Claisen–Schmidt chemistry, a large variety of different HBA ring combinations was accessible, which were expected to have a strong impact on the potency and selectivity profile due to differences in lipophilicity, acidity and molecular

electrostatic potentials. Since a systematic study of the most straightforward combinations had not been done before, we decided to synthesize and explore a set of new scaffolds exhibiting the minimum pharmacophore features according to

Figure 2. In order to maintain a good probability of CNS penetration, the molecular weight was kept below 280 g/mol.

Table 1. Inhibitory activity of α -benzylidene- γ -butyrolactone derivatives against Dyrk1A and selectivity profiling against a panel of selected kinases.

#	Structure	(IC50, μ M) ^a						
		D1A	D1B	D2	CK2	Clk1	EGFR	PKC β
1		1.81	3.80	>10	n.i.	>10	n.i.	n.i.
2		0.93	6.70	>10	>10	3.90	>10	n.i.
3		1.10	5.80	>10	>10	7.52	n.i.	n.i.
4		1.20	10.5	n.i.	>10	4.37	n.d.	n.i.
5		0.96	2.17	0.82	>10	>10	>10	n.i.
6		0.17	2.64	0.43	>10	>10	>10	n.i.
7		0.13	1.05	0.06	>10	>10	>10	n.i.
8		0.88	4.29	2.04	>10	>10	>10	n.i.
9		0.60	2.63	0.99	>10	>10	>10	n.i.
10		1.08	1.68	>10	>10	0.17	>10	n.i.
Hrm		0.13	0.18	3.00	n.d.	0.22	n.d.	n.d.

^aS.D. \leq 18%, [ATP]=100 μ M; D1A=Dyrk1A, D1B=Dyrk1B, D2=Dyrk2; Hrm=Harminine; n.i., no inhibition; n.d., not determined.

2.2. Structure-Activity relationships (SAR)

First, several γ -butyrolactone moieties were combined with different benzylidene units, and the influence on potency and selectivity was tested. The kinases chosen for the primary screening panel were (i) frequently reported off-targets for diverse classes of Dyrk1A inhibitors (first five kinases in Tables 1 and 2, all from the CMGC family) [21], and (ii) kinases from more distant families (last two in Tables 1 and 2). In this way, conclusive selectivity data were immediately obtained.

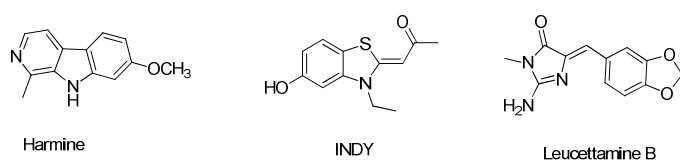


Figure 1. 2D structures of harminine, INDY and Leucettamine B.

The first synthesized compound **1** was moderately active as Dyrk1A inhibitor (Table 1) and quite selective against our panel of kinases. It did not appreciably inhibit Dyrk2 and showed weaker activity even against Dyrk1B. In order to increase its activity and selectivity, we decided to rigidify the *p*-methoxybenzene into a chromane (compound **2**). This non-planar, partially saturated system was favorable for the inhibition of Dyrk1A but less well tolerated by Dyrk1B, resulting in increased selectivity towards the latter isoform. This modification may take advantage – at least indirectly – of the only difference between the ATP binding pockets of Dyrk1A and Dyrk1B, which is the exchange of the linear side chain of hinge region residue Met240 in Dyrk1A by a branched leucine in Dyrk1B. Although pointing away from the ATP pocket, the Leu side chain might restrict the flexibility of some β -sheet residues that form the lid of the pocket to adapt to sterically more demanding cyclic moieties. An extension of the lactone ring to a six-membered cycle (**3**) or by a methyl substituent (**4**) confirmed the trend that the ATP-binding

pocket of Dyrk1A accepts more bulky structures than that of Dyrk1B, as indicated by the 9 times higher potency of **4** for Dyrk1A. Consistent with this finding, the less bulky coumaran moiety in **5** caused a drop of the selectivity towards Dyrk1B (compared with **2**) – and particularly towards Dyrk2 –, while the inhibition of Dyrk1A was conserved. Reintroducing a methyl substituent in **6** not only recovered the selectivity toward Dyrk1B but markedly increased the potency toward Dyrk1A (IC₅₀: 0.17 μM). Thus, the potency was similar to that of harmine but the selectivity towards Dyrk1B was considerably improved, reaching a remarkable selectivity factor of 15.5 (cf. Table 1). The 5-methyl substituent in **6** increased the selectivity in general, which became particularly evident from the negligible inhibition of the atypical kinase haspin by **6** (43% at 5 μM) compared to **7** (75% at 5 μM) (Table 3). Haspin was reported as a notorious off-target even for some of the most selective Dyrk1A inhibitors, including TG003 and harmine [27,33]. An extended selectivity profiling for compound **6** revealed that besides Dyrk1A and Clk1, only Clk4 was affected in our panel (Table S1, Supplementary Material). The IC₅₀ for Clk4 as determined by the LanthaScreen® Kinase Binding Assay was 32 nM. However, this assay is based on the competition of the test compound with an Alexa Fluor®-conjugated tracer compound for binding to the ATP site, thus the IC₅₀ is difficult to compare with IC₅₀s obtained by peptide

phosphorylation assays. The next most strongly inhibited kinase was PI3Kα, with an IC₅₀ of 0.65 μM (determined by a substrate phosphorylation assay in the presence of 100 μM ATP). The PI3 lipid kinases had been included in the screening panel for reasons stated below.

Because **6** still significantly inhibited Clk1 (and probably Clk4), we tried to further optimize the selectivity by modifying the benzylidene part of the molecule. Our strategy of including a second oxygen atom was unsuccessful as both potency and selectivity decreased (cf. compounds **8** and **9**). Subsequently, we decided to replace the coumaran of compound **5** by a benzothiazole moiety, leading to a potent inhibitor (**7**) with dual selectivity for Dyrk1A and Clk1. Surprisingly, our attempt to further increase the potency and selectivity for Dyrk1A by introducing a methyl on the γ-butyrolactone ring failed (compound **10**). Probably the methyl group forced the compound into a slightly different binding orientation, which negatively affected the H-bond interaction between the benzothiazole nitrogen and the hinge region. The distinct behavior of compound **6** might be explained by the different spatial orientation of the oxygen lone pairs. However, the affinity to Clk1 was less affected, thus rendering compound **10** moderately selective for Clk1.

Table 2. Inhibitory activity of benzylidene thioxothiazolidinone-based derivatives against Dyrk1A and selectivity profiling against a panel of selected kinases.

#	A	B	D1A	D1B	D2	CK2	Clk1	EGFR	PKCβ
			(IC ₅₀ , μM) ^a						
11			>10	n.d.	n.d.	n.d.	n.d.	n.d.	n.d.
12			6.4	>10	n.i.	n.i.	10	n.d.	n.i.
13			1.3	5.2	9.2	0.17	3.6	n.i.	n.i.
14			0.25	1.5	>10	0.22	5.7	n.i.	n.i.
15			0.1	0.3	1.0	0.1	0.5	>10	>10
16			0.04	0.07	0.20	0.06	0.1	>10	9.2
17			0.02	0.06	0.06	0.04	0.2	>10	>10
18			0.7	0.9	1.5	2.4	0.02	>10	>10
AS			0.03	0.08	0.1	0.02	0.07	>10	n.i.

^aS.D.≤18%, [ATP]=100μM; D1A=Dyrk1A, D1B=Dyrk1B, D2=Dyrk2, AS= AS605240; n.d., not determined; n.i., no inhibition.

Our second set of compounds (Table 2) was designed by modifying the lactone part of the molecule in order to establish stronger interactions in the binding site and thus boost the potency. For the first compounds, we decided to use again 4-methoxybenzaldehyde as coupling partner, since the plain methoxy substituent on the benzene had conferred the highest selectivity towards Clk1 so far (cf. compounds **1** and **3** in Table 1). The first designed compound **11** was not active, suggesting that the combination of two carbonyls in the pyrrolidinedione was too polar for the binding site (Table 2). Similarly, the hydantoin derivative **12** exhibited only a weak inhibitory activity toward Dyrk1A. Nonetheless, when the NH heteroatom unit was replaced by sulfur leading to the thiazolidinedione ring, appreciable inhibition was observed (compound **13**). Interestingly, **13** was mainly selective for CK2, exhibiting an IC_{50} of 0.17 μ M. Since CK2 is known to preferably bind acidic compounds in the ATP-binding site [34,35], the relatively low pKa value of the thiazolidinedione group (reported to be 6.14 for the unsubstituted analog [36]) may account for this selectivity. Indeed, the NH acidity of the CK2-inactive analog **12** is considerably lower (pKa value: 8.9 [37]). We further explored the effects of sulfur atoms by incorporating the rhodanine system (2-thioxothiazolidin-4-one). This resulted in 5-fold increase in the Dyrk1A inhibitory potency (compare compound **14** with **13**), while the CK2 inhibition remained unchanged. This was again in accordance with the acidic pKa of **14**, which was previously reported to be 5.8 [38]. Thus, **14** was a dual inhibitor of Dyrk1A and CK2; of note, the overall selectivity did not drop, even though the rhodanine system was frequently present in hits identified for many different enzymes [39]. In particular, the high selectivity (23-fold) of **14** over Clk1 was remarkable. CK2 is also believed to be involved in the pathology of Alzheimer's disease [40–42]. Thus, **14** might allow to evaluate whether simultaneous inhibition of Dyrk1A and CK2 has any benefit in Alzheimer's disease models without significantly affecting Clk1.

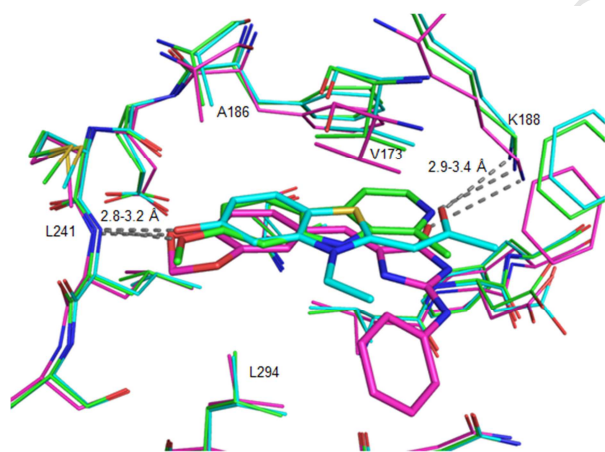


Figure 2. Superimposition of harmine (green), INDY (cyan) and Leucettine L41 (magenta) cocrystallized with Dyrk1A (PDB codes 3ANR, 3ANQ and 4AZE, respectively). All ligands are bound in the ATP-binding cleft *via* two H-bonds, formed with Leu241-NH at the hinge region and Lys188 (indicated by the grey dashed lines). The measured ranges of the N–O distances are given in Å. Additional contacts comprise van der Waals-interactions with the side chains of Ala186, Val173 and Leu294, which mainly involve the left aromatic rings.

In the course of our study, we found that the selectivity of the rhodanine moiety was strongly modulated by the extent of the aromatic system. The selectivity toward Dyrk1B and Dyrk2 was reduced stepwise when the coumaran (**15**) and particularly the

benzothiazole (**16**) and quinoline (**17**) rings were introduced. The resulting nanomolar inhibitors **16** and **17** were multi-targeted within the CMGC kinase family, but not promiscuous, since PKC β and EGFR kinase were not affected.

Because the benzothiazole moiety in **16** generated a moderate selectivity over Dyrk2, it was also combined with thiohydantoin (cpd. **18**) to test whether this favorable inhibitory profile and the potency of the rhodanine analog **16** might be retained. While the activities against Dyrk1A and CK2 dropped, compound **18** displayed an impressive selectivity for Clk1 (35 fold over Dyrk1A). Thus, our scaffold diversification identified thiohydantoin as a novel moiety mediating strong and selective affinity for Clk1.

Because of the obvious structural similarity of our compounds **16** and **17** with the thiazolidinedione AS605240 (Table 2), which was previously described as a rather selective PI3K γ inhibitor (IC_{50} : 8 nM) [43], it was straightforward to enlarge our panel of screened kinases by some of the PI3K isoforms; in turn, we tested AS605240 against our kinase targets. Indeed, AS605240 turned out to be a nanomolar inhibitor of Dyrk1A and CK2 as well (Table 2), and not surprisingly, both **16** and **17** were highly active against PI3K γ and $-\alpha$ (Table 3). Compound **17** was slightly more selective than **16**, exhibiting lower activity toward PI3K δ and Clk1 (Tables 2 and 3; see also extended screening in Table S1, Supplementary Material). Of note, both for **16** and **17**, a reduced activity against the atypical kinase haspin was noted (Table 3), corroborating that the rhodanine moiety does not *a priori* confer non-specific behaviour. Collectively, we identified CK2 α , Clk1, STK17A and PI3K α/γ as additional targets for **16** and **17** (Tables 2, 3 and S1), of which, however, PI3K α/γ turned out to be most potently inhibited. Literature data on the pathogenic roles of these kinases in glioma suggest that they can all be considered as potential targets in this brain malignancy (Table S2, Supplementary Material). In light of this, the compounds presented here might display a favorable profile as multi-target agents for the treatment of glioma. Indeed, we found that **16**, **17** and AS605240 inhibited the growth of U87MG glioma cells with submicromolar IC_{50} s, being more potent than the rather Dyrk1A/1B-selective reference compound harmine (Table S3, Supplementary Material).

Table 3. Extended selectivity profiling of **16** and **17**.

Kinase	16	17
	IC_{50} (nM) ^b	
STK17A (DRAK1)	n.d.	12.8
PIM1	n.d.	103
Haspin	255 (93% ^a)	259 (93% ^a)
PI3K-C2 β	56% ^a	62% ^a
PI3K-p110- α	2.2	2.6
PI3K-p110- δ	12.4	16.1
PI3K-p110- γ	2.3	2.3

^a% inhibition at 1 μ M; shown are mean values of two different measurements performed in duplicates (S.D. \leq 2.5%); ^b IC_{50} s were only determined when the % inhibition at 1 μ M was greater than 85%. Data were calculated based on mean values of duplicates that differed by less than 7%.

To the best of our knowledge, this is the first report showing that AS605240 is a strong inhibitor of Dyrk1A, CK2 and Clk1,

and that dual inhibitors of PI3 lipid kinases and protein kinases can be developed. However, inhibition of multiple kinases might be associated with severe side effects. In this regard, it is noteworthy that AS605240, which exhibits an *in vitro* inhibitory profile similar to **16** and **17**, found a widespread use in many murine models of inflammatory diseases, including rheumatoid arthritis, systemic lupus erythematosus, atherosclerosis, colitis, liver fibrosis and pulmonary fibrosis [44–46]. No signs of toxicity were observed in any of these studies, even though some used high oral dosage, e. g., 50 mg/kg twice per day over 14 days [44]. Moreover, in a xenograft model using PI3K γ -expressing neuroblastoma cells in SCID mice, AS605240 effectively suppressed tumor growth at 20 mg/kg [47]. In the light of our findings – although the inhibition of PI3K γ may account for a large part of the observed therapeutic effects – it is fair to ask retrospectively what contribution was made by the inhibition of the kinase targets that were identified for AS605240 in our screening, Dyrk1A, CK2 α and Clk1. At any rate, the absence of toxic effects of AS605240 proves that in rodents, multi-targeted inhibitions involving even a pleiotropic kinase such as CK2, are not harmful to the organism, at least in short-term treatments.

Having discovered new Dyrk1A inhibitory scaffolds with diverse selectivity profiles, we were interested to evaluate their potency to inhibit the Dyrk1A-catalyzed tau phosphorylation in intact cells. To this end, we used a HEK293 cell line which overexpressed both Dyrk1A and human tau protein. Under the chosen conditions, phosphorylation of tau at Thr212 is solely dependent on the Dyrk1A activity [48]. Testing of the most potent Dyrk1A inhibitors from Tables 1 and 2, **6**, **7**, **16** and **17**, along with AS605240, revealed that the tau phosphorylation was suppressed at low micromolar and sub-micromolar concentrations (Figure 3). There was no obvious correlation with the inhibitory activities of the compounds against purified Dyrk1A, since the most potent compounds in the cell free assay, **16**, **17** and **AS506240** were inferior to harmine and compound **7**. Probably the distinct physicochemical properties of the scaffolds accounted for variable degrees in cell permeability and further pharmacokinetic properties. The high cellular potency of **7** was encouraging, suggesting that benzothiazolylmethylene- γ -butyrolactone might be a suitable core structure for the development of novel therapeutic agents against Alzheimer's disease and also against diseases involving abnormal pre-mRNA splicing, since Clk1 was strongly co-inhibited by **7** in the cell free assay (Table 1). Given the low molecular weight (231.3 g/mol), the small polar surface area (tPSA= 38.66 Å²) and the absence of H-bond donors, the compound fulfills the major criteria for CNS availability [31].

However, most of our new scaffolds exhibited two metabolically weak spots, which might impede *in vivo* applications. One was the lactone ring structure, which might be hydrolyzed by esterases present in the serum and/or cells, and the other one was the potential Michael acceptor motif, which may also have toxicological implications. The Michael-type acceptor reactivity of some of the scaffolds disclosed as kinase inhibitors in this study, including 5-benzylidene thiazolidinediones, hydantoins, thiohydantoins and rhodanines, had been analyzed previously by Arsovska et al [49]. The authors found that the 5-benzylidene five-membered oxo-heterocycles revealed almost insignificant reactivity toward cysteamine as an exemplary biological nucleophile.

Hydrolytic instability was mainly a concern for the lactone derivatives in Table 1. Therefore we decided to test the stability of some selected compounds in rat plasma. As reference compounds, diltiazem and *N*-acetyl-*L*-phenylalanine ethyl ester

were chosen, possessing a plasma-stable [50] and a labile ester function [51], respectively. As can be seen from Table 4, all analyzed compounds exhibited a long half-life in rat plasma, similar to or better than that of diltiazem ($t_{1/2}$ = 125 min), indicating a high metabolic stability in plasma. In contrast, *N*-acetyl-*L*-phenylalanine ethyl ester was completely metabolized within a few minutes, as it was expected. Thus, it can be concluded that the lactone and lactam rings of our compounds are not hydrolyzed by plasma enzymes.

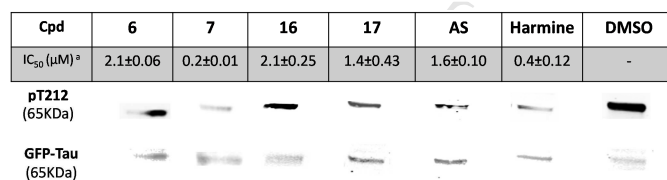


Figure 3. Inhibition of Dyrk1A-catalyzed tau-Thr212 phosphorylation in stably transfected HEK293 cells. The test compounds, DMSO or the reference inhibitor harmine [54] were added to the cell medium and the Dyrk1A expression induced as described. After immunoblotting of the total cell proteins, the level of phospho-tau-Thr212 was detected using a phosphospecific antibody. To normalize the signals, total recombinant GFP-tau protein was quantified on the same blot using an anti-GFP antibody (fluorescence image converted to grey scales). Initial screenings were performed at 1 μM compound concentrations (lower panel; one representative experiment out of two is shown). ¹⁴C₅₀ values were determined after cell treatment with different concentrations in triplicates, referring to the signal derived from DMSO-treated cells as 100%. Values represent averages from at least two independent determinations (±S.D.); AS, AS605240.

3. Conclusions

Systematic variation of benzylidene-coupled heterocycles, differing in acceptor strength, lipophilicity and electrostatic potential, was highly effective to generate new scaffolds with different kinase selectivities and potencies, while keeping the molecular weight below 280 g/mol. Although we could not provide experimental evidence for a blood-brain-barrier penetration of our inhibitors within the scope of this study, the close structural similarity to some benzylidene derivatives previously reported to be brain-permeable suggests that at least some of our lead compounds might share this property, including the benzylidene hydantoins (similar to compound **28** in [52]) and the thiazolidinediones that are structurally similar to AS605240 [53].

With respect to novel agents against neurodegenerative diseases, compound **7** displayed the most promising activity in our cell-based tau phosphorylation assay. In a cytotoxicity assay, **7** was not toxic toward HEK293 cells at concentrations up to 20 μM (data not shown). The compound might be useful as a tool to further explore the effects of co-inhibition of Dyrk1A and Clk1/4 on the pathogenic mechanisms of Alzheimer's disease. Other compounds, such as **3** and **4**, were not very potent but showed an appreciable selectivity towards Dyrk1B and Clk1. These compounds might be considered as elaborated, selective fragments with still good ligand efficiencies (0.55 and 0.54, respectively). In order to optimize the potency, they might be extended analogously to the leucettines, through functionalization e. g., at position 5 of the γ -butyrolactone in **4**.

Within our panel of frequent off-target kinases for Dyrk1A inhibitors, the thiazolidinedione **13** and thiohydantion **18** were selective for CK2, probably because of their elevated acidity. The presence of thione sulfur in the five-membered ring generally increased the potency, however, mostly at the expense of selectivity. The loss of selectivity remained limited when the aromatic portion of the benzylidene moiety was restricted to a single ring (cf. compounds **14** and **16**). Upon introducing a bicyclic aromatic system, however, the selectivity toward Dyrk1B, Dyrk2 and CK2 was abolished, yielding potent, multi-targeted inhibitors with enhanced anti-proliferative effect on the U87MG glioma cell line (Table S3, Supplementary Material). Interestingly, this class of compounds included the widely studied AS605240, formerly reported as rather selective PI3K γ inhibitor. Altogether, our results showed that inhibitors which simultaneously target PI3 kinases and oncogenic protein kinases can be developed, with potential benefit in anti-cancer applications.

Table 4. Metabolic stability in rat plasma.

Compound	$t_{1/2}$ in rat plasma [min] ^a
6	>> 120 ^b
5	>> 120 ^b
7	186
16	101
Diltiazem	125
<i>N</i> -acetyl- <i>L</i> -phenylalanine ethyl ester	< 5

^amean values from two experiments, S.D.< 17%; ^bno degradation detected after 120 min

4. Methods

4.1. Chemistry. Synthesis of the key compounds **6**, **16** and **17**

Synthesis of (*E*)-3-((2,3-dihydrobenzofuran-5-yl)methylene)-5-methylidihydrofuran-2(3*H*)-one (**6**)

To a solution of NaH in dry toluene (0.162 g, 4.05 mmol), a solution of the δ -valerolactone (0.324 g, 3.24 mmol, 0.309 mL) was added, and the mixture stirred overnight at room temperature. On the next day, the mixture was cooled in an ice bath and 2,3-dihydrobenzo-furan-5-carboxaldehyde (0.300 g, 2.025 mmol) dissolved in dry toluene was added dropwise. The temperature was slowly increased to reflux until the starting materials were consumed. After cooling down, a solution of 10% H₂SO₄ was added and the solution stirred at room temperature for few minutes. Then 10 mL of water were added and the mixture extracted 3 times with ethyl acetate (10 mL). The organic phase was washed with brine and dried over Na₂SO₄. After evaporating the solvent *in vacuo*, crude product was purified the column chromatography. Yield: 31%. Mp: 131°C. ¹H NMR (500 MHz, DMSO-*d*₆) δ ppm 1.36 (d, J=6.31 Hz, 3 H) 2.72 - 2.84 (m, 1 H) 3.23 (t, J=8.67 Hz, 2 H) 3.33 - 3.40 (m, 1 H) 4.60 (t, J=8.67 Hz, 2 H) 4.69 - 4.79 (m, 1 H) 6.87 (d, J=8.20 Hz, 1 H) 7.35 (s, 1 H) 7.37 - 7.41 (m, 1 H) 7.51 (s, 1 H). ¹³C NMR (126 MHz, DMSO-*d*₆) δ ppm 22.03 (s, 1 C) 28.66 (s, 1 C) 34.63 (s, 1 C) 71.66 (s, 1 C) 73.64 (s, 1 C) 109.37 (s, 1 C) 122.20 (s, 1 C) 126.72 (s, 1 C) 127.18 (s, 1 C) 128.47 (s, 1 C) 131.34 (s, 1 C) 135.15 (s, 1 C) 161.17 (s, 1 C) 171.65 (s, 1 C). LC-MS (ESI): *m/z* MH⁺ = 231.

General procedure A: rhodanine or hydantoin (1 eq), the corresponding aldehyde (1 eq) and sodium acetate (3 eq) were dissolved in 5 ml of acetic acid and the solution heated at 110°C, if necessary under microwave conditions (130W for ~10 minutes). After cooling, the precipitate was filtered off, washed to remove all the acetic acid and dried *in vacuo*. The reaction has been described in Mendgen et al[39] to be stereospecific producing the *Z*-isomer as confirmed by the single peak in the HPLC.

Synthesis of (*Z*)-5-(benzo[*d*]thiazol-6-ylmethylene)-2-thioxothiazolidin-4-one (**16**)

Rhodanine (0.254 g, 1.84 mmol), 1,3-benzothiazole-6-carbaldehyde (0.300 g, 1.84 mmol) and sodium acetate (0.452 g, 5.51 mmol) were used following the general procedure A described above. Yield: 2%. Mp: > 300°C. ¹H NMR (500 MHz, DMSO-*d*₆) δ ppm 7.76 (d, J=8.51 Hz, 1 H) 7.78 (s, 1 H) 8.21 (d, J=8.51 Hz, 1 H) 8.47 (s, 1 H) 9.50 - 9.58 (m, 1 H) 13.88 (br. s., 1 H). ¹³C NMR (126 MHz, DMSO-*d*₆) δ ppm 123.74 (s, 1 C) 125.09 (s, 1 C) 125.97 (s, 1 C) 128.30 (s, 1 C) 130.26 (s, 1 C) 131.13 (s, 1 C) 134.94 (s, 1 C) 153.93 (s, 1 C) 159.56 (s, 1 C) 169.43 (s, 1 C) 195.71 (s, 1 C). LC-MS (ESI): *m/z* MH⁺ = 279.

Synthesis of (*Z*)-5-(quinolin-6-ylmethylene)-2-thioxothiazolidin-4-one (**17**)

Rhodanine (0.254 g, 1.909 mmol), 6-quinoline-carbaldehyde (0.300 g, 1.909 mmol) and sodium acetate (0.470 g, 5.73 mmol) were used following the general procedure A described above. Yield: 90%. Mp: >300°C. ¹H NMR (500 MHz, DMSO-*d*₆) δ ppm 7.62 (dd, J=8.35, 4.26 Hz, 1 H) 7.82 (s, 1 H) 7.95 (dd, J=8.83, 2.21 Hz, 1 H) 8.13 (d, J=8.83 Hz, 1 H) 8.24 (d, J=2.21 Hz, 1 H) 8.52 - 8.56 (m, 1 H) 8.98 (dd, J=4.26, 1.73 Hz, 1 H) 13.69 - 14.22 (m, 1 H). ¹³C NMR (126 MHz, DMSO-*d*₆) δ ppm 122.53 (s, 1 C) 126.93 (s, 1 C) 127.13 - 128.39 (m, 1 C) 130.06 (s, 1 C) 130.25 - 130.44 (m, 1 C) 130.55 - 130.76 (m, 1 C) 131.03 (s, 1 C) 131.15 (s, 1 C) 136.95 (s, 1 C) 147.74 (s, 1 C) 152.34 (s, 1 C) 169.45 (s, 1 C) 195.72 (s, 1 C) LC-MS (ESI): *m/z* MH⁺ = 273.

4.2. Biology

Kinase assay. Inhibition assays for Dyrk1A, Dyrk1B, Dyrk2, CK2alpha, Clk1, EGFR and PKCβ were performed using purified recombinant kinase protein in the presence of 100 μM ATP as described previously [29].

HEK293-tau-Dyrk1A cell assay. The cell line was developed, and the assays for the inhibition of cellular Dyrk1A activity were performed as described previously[48]. In brief, HEK293-tau-Dyrk1A cells which stably overexpress EGFP-fused human full length tau protein and tetracycline-inducible EGFP-fused Dyrk1A were grown in 12-well plates to 70% confluency; then tetracycline (0.3 μg/mL) and test compounds were added from stock solutions. The next day, the cells were lysed and the lysates analyzed by immunoblotting using an anti-phospho-tau-Thr212 antibody (pT212, Life Technologies GmbH, Cat No. 444-740g, dil. 1:1000) and a mouse anti-GFP antibody (Life Technologies GmbH, Cat. No. 33-2600, dil. 1:1000) for normalization of the signals. After incubation with dye-labeled secondary antibodies, the signals for pT212 and EGFP were simultaneously detected using an Odyssey infrared imager (LI-COR). Figure 3 shows the image converted to grey scales.

Metabolic stability tests in rat plasma. The test or reference compounds (1 μM) were incubated with rat plasma (pooled, heparinized) at 37 °C for 0, 5, 15, 30, 60, and 120 min. The incubation was stopped by precipitation of plasma proteins with 5 volumes of cold acetonitrile containing an internal standard, and the remaining compound concentration was analyzed by LC-MS/MS. N-Acetyl-L-phenylalanine ethyl ester (Cat. No. A4251) and diltiazem hydrochloride (Cat. No. D2521) were from Sigma.

Calculation of ligand efficiency. The calculations were done by dividing the Gibbs free energy of binding by the number of non-hydrogen atoms. K_i values were calculated from the IC_{50} s using the Cheng-Prussoff equation. The K_M value of our Dyrk1A preparation for ATP was previously determined to be 64 μM [29].

Bibliography

- [1] S. Aranda, A. Laguna, S. de la Luna, DYRK family of protein kinases: evolutionary relationships, biochemical properties, and functional roles, *FASEB J.* 25 (2011) 449–462. doi:10.1096/fj.10-165837.
- [2] W.J. Song, L.R. Sternberg, C. Kasten-Sportès, M.L. Keuren, S.H. Chung, A.C. Slack, D.E. Miller, T.W. Glover, P.W. Chiang, L. Lou, D.M. Kurmit, Isolation of human and murine homologues of the *Drosophila* minibrain gene: human homologue maps to 21q22.2 in the Down syndrome “critical region”, *Genomics* 38 (1996) 331–339. doi:10.1006/geno.1996.0636.
- [3] R. Kimura, K. Kamino, M. Yamamoto, A. Nuripa, T. Kida, H. Kazui, R. Hashimoto, T. Tanaka, T. Kudo, H. Yamagata, Y. Tabara, T. Miki, H. Akatsu, K. Kosaka, E. Funakoshi, K. Nishitomi, G. Sakaguchi, A. Kato, H. Hattori, T. Uema, M. Takeda, The DYRK1A gene, encoded in chromosome 21 Down syndrome critical region, bridges between beta-amyloid production and tau phosphorylation in Alzheimer disease, *Hum. Mol. Genet.* 16 (2007) 15–23. doi:10.1093/hmg/ddl437.
- [4] Y.L. Woods, P. Cohen, W. Becker, R. Jakes, M. Goedert, X. Wang, G.C. Proud, The kinase DYRK phosphorylates protein-synthesis initiation factor eIF2Bepsilon at Ser539 and the microtubule-associated protein tau at Thr212: potential role for DYRK as a glycogen synthase kinase 3-priming kinase, *Biochem. J.* 355 (2001) 609–615.
- [5] F.J. Tejedor, B. Hämmerle, MNB/DYRK1A as a multiple regulator of neuronal development, *FEBS J.* 278 (2011) 223–235. doi:10.1111/j.1742-4658.2010.07954.x.
- [6] N. Pozo, C. Zahonero, P. Fernández, J.M. Liñares, A. Ayuso, M. Hagiwara, A. Pérez, J.R. Ricoy, A. Hernández-Lafín, J.M. Sepúlveda, P. Sánchez-Gómez, Inhibition of DYRK1A destabilizes

EGFR and reduces EGFR-dependent glioblastoma growth, *J. Clin. Invest.* 123 (2013) 2475–2487. doi:10.1172/JCI63623.

- [7] S. Agarwal, R.K. Mittapalli, D.M. Zellmer, J.L. Gallardo, R. Donelson, C. Seiler, S.A. Decker, K.S. Santacruz, J.L. Pokorny, J.N. Sarkaria, W.F. Elmquist, J.R. Ohlfest, Active efflux of Dasatinib from the brain limits efficacy against murine glioblastoma: broad implications for the clinical use of molecularly targeted agents, *Mol. Cancer Ther.* 11 (2012) 2183–2192. doi:10.1158/1535-7163.MCT-12-0552.
- [8] S. Aranda, M. Alvarez, S. Turró, A. Laguna, S. de la Luna, Sprouty2-mediated inhibition of fibroblast growth factor signaling is modulated by the protein kinase DYRK1A, *Mol. Cell. Biol.* 28 (2008) 5899–5911. doi:10.1128/MCB.00394-08.
- [9] S.R. Ferron, N. Pozo, A. Laguna, S. Aranda, E. Porlan, M. Moreno, C. Fillat, S. de la Luna, P. Sánchez, M.L. Arbonés, I. Fariñas, Regulated segregation of kinase Dyrk1A during asymmetric neural stem cell division is critical for EGFR-mediated biased signaling, *Cell Stem Cell.* 7 (2010) 367–379. doi:10.1016/j.stem.2010.06.021.
- [10] Y.L. Woods, G. Rena, N. Morrice, A. Barthel, W. Becker, S. Guo, T.G. Unterman, P. Cohen, The kinase DYRK1A phosphorylates the transcription factor FKHR at Ser329 in vitro, a novel in vivo phosphorylation site, *Biochem. J.* 355 (2001) 597–607.
- [11] H.S. Chang, C.H. Lin, C.H. Yang, M.S. Yen, C.R. Lai, Y.R. Chen, Y.L. Liang, W.C. Yu, Increased expression of Dyrk1a in HPV16 immortalized keratinocytes enable evasion of apoptosis, *Int. J. Cancer.* 120 (2007) 2377–2385. doi:10.1002/ijc.22573.
- [12] S.L. Pomeroy, P. Tamayo, M. Gaasenbeek, L.M. Sturla, M. Angelo, M.E. McLaughlin, J.Y.H. Kim, L.C. Goumnerova, P.M. Black, C. Lau, J.C. Allen, D. Zazag, J.M. Olson, T. Curran, C. Wetmore, J.A. Biegel, T. Poggio, S. Mukherjee, R. Rifkin, A. Califano, G. Stolovitzky, D. N. Louis, J.P. Mesirov, E.S. Lander, T.R. Golub, Prediction of central nervous system embryonal tumour outcome based on gene expression, *Nature* 415 (2002) 436–442. doi:10.1038/415436a.
- [13] R. Shai, T. Shi, T.J. Kremen, S. Horvath, L.M. Liau, T.F. Cloughesy, P.S. Mischel, S.F. Nelson, Gene expression profiling identifies molecular subtypes of gliomas, *Oncogene* 22 (2003) 4918–4923. doi:10.1038/sj.onc.1206753.
- [14] J. Shi, T. Zhang, C. Zhou, M.O. Chohan, X. Gu, J. Wegiel, J. Zhou, Y.W. Hwang, K. Iqbal, I. Grundke-Iqbal, C.X. Gong, F. Liu, Increased dosage of Dyrk1A alters alternative splicing factor (ASF)-regulated alternative splicing of tau in Down syndrome, *J. Biol. Chem.* 283 (2008) 28660–28669. doi:10.1074/jbc.M802645200.
- [15] W. Qian, H. Liang, J. Shi, N. Jin, I. Grundke-Iqbal, K. Iqbal, C.X. Gong, F. Liu, Regulation of the alternative splicing of tau exon 10 by SC35 and Dyrk1A, *Nucleic Acids Res.* 39 (2011) 6161–6171. doi:10.1093/nar/gkr195.
- [16] X. Yin, N. Jin, J. Gu, J. Shi, J. Zhou, C.-X. Gong, K. Iqbal, I. Grundke-Iqbal, F. Liu, Dual-specificity tyrosine phosphorylation-regulated kinase 1A (Dyrk1A) modulates serine/arginine-rich protein 55 (SRp55)-promoted Tau exon 10 inclusion, *J. Biol. Chem.* 287 (2012) 30497–30506. doi:10.1074/jbc.M112.355412.
- [17] A.M. Hartmann, D. Rujescu, T. Giannakouros, E. Nikolakaki, M. Goedert, E.M. Mandelkow, Q.S. Gao, A. Andreadis, S. Stamm, Regulation of alternative splicing of human tau exon 10 by phosphorylation of splicing factors, *Mol. Cell. Neurosci.* 18 (2001) 80–90. doi:10.1006/mcne.2001.1000.
- [18] P. Jain, C. Karthikeyan, N.S. Hari Narayana Moorthy, D. Kumar Waiker, A. Kumar Jain, P. Trivedi, Human CDC2-Like Kinase 1 (CLK1): A Novel Target for Alzheimer’s Disease, *Curr. Drug Targets* 15 (2014) 539–550.
- [19] S. Stamm, S. Ben-Ari, I. Rafalska, Y. Tang, Z. Zhang, D. Toiber, T.A. Thanaraj, H. Soreq, Function of alternative splicing, *Gene* 344 (2005) 1–20. doi:10.1016/j.gene.2004.10.022.
- [20] T. Misteli, J.F. Cáceres, J.Q. Clement, A.R. Krainer, M.F. Wilkinson, D.L. Spector, Serine phosphorylation of SR proteins is required for their recruitment to sites of transcription in vivo, *J. Cell Biol.* 143 (1998) 297–307.
- [21] C. Schmitt, P. Miralinaghi, M. Mariano, R.W. Hartmann, M. Engel, Hydroxybenzothioephene Ketones Are Efficient Pre-mRNA

- [22] M. Debdab, F. Carreaux, S. Renault, M. Soundararajan, O. Fedorov, P. Filippakopoulos, O. Lozach, L. Babault, T. Tahtouh, B. Baratte, Y. Ogawa, M. Hagiwara, A. Eisenreich, U. Rauch, S. Knapp, L. Meijer, J.P. Bazureau, Leucettines, a class of potent inhibitors of cdc2-like kinases and dual specificity, tyrosine phosphorylation regulated kinases derived from the marine sponge leucettamine B: modulation of alternative pre-RNA splicing, *J. Med. Chem.* 54 (2011) 4172–4186. doi:10.1021/jm200274d.
- [23] G. Naert, V. Ferré, J. Meunier, E. Keller, S. Malmström, L. Givalois, F. Carreaux, J.P. Bazureau, T. Maurice, Leucettine L41, a DYRK1A-preferential DYRKs/CLKs inhibitor, prevents memory impairments and neurotoxicity induced by oligomeric Aβ₂₅₋₃₅ peptide administration in mice, *Eur. Neuropsychopharmacol.* 25 (2015) 2170–2182. doi:10.1016/j.euroneuro.2015.03.018.
- [24] W. Becker, U. Soppa, F.J. Tejedor, DYRK1A: a potential drug target for multiple Down syndrome neuropathologies, *CNS Neurol. Disord. Drug Targets.* 13 (2014) 26–33.
- [25] C. Kuhn, D. Frank, R. Will, C. Jaschinski, R. Frauen, H.A. Katus, N. Frey, DYRK1A is a novel negative regulator of cardiomyocyte hypertrophy, *J. Biol. Chem.* 284 (2009) 17320–17327. doi:10.1074/jbc.M109.006759.
- [26] Y. Ogawa, Y. Nonaka, T. Goto, E. Ohnishi, T. Hiramatsu, I. Kii, M. Yoshida, T. Ikura, H. Onogi, H. Shibuya, T. Hosoya, N. Ito, M. Hagiwara, Development of a novel selective inhibitor of the Down syndrome-related kinase Dyrk1A, *Nat. Commun.* 1 (2010) 86. doi:10.1038/ncomms1090.
- [27] O. Fedorov, K. Huber, A. Eisenreich, P. Filippakopoulos, O. King, A.N. Bullock, D. Szklarczyk, L.J. Jensen, D. Fabbro, J. Trappe, U. Rauch, F. Bracher, S. Knapp, Specific CLK inhibitors from a novel chemotype for regulation of alternative splicing, *Chem. Biol.* 18 (2011) 67–76. doi:10.1016/j.chembiol.2010.11.009.
- [28] T. Tahtouh, J.M. Elkins, P. Filippakopoulos, M. Soundararajan, G. Burgy, E. Durieu, C. Cochet, R.S. Schmid, D.C. Lo, F. Delhomme, A.E. Oberholzer, L.H. Pearl, F. Carreaux, J.P. Bazureau, S. Knapp, L. Meijer, Selectivity, cocrystal structures, and neuroprotective properties of leucettines, a family of protein kinase inhibitors derived from the marine sponge alkaloid leucettamine B, *J. Med. Chem.* 55 (2012) 9312–9330. doi:10.1021/jm301034u.
- [29] C. Schmitt, D. Kail, M. Mariano, M. Empting, N. Weber, T. Paul, R.W. Hartmann, M. Engel, Design and synthesis of a library of lead-like 2,4-bis(heterocyclic) substituted thiophenes as selective Dyrk/Clk inhibitors, *PLoS One.* 9 (2014) e87851. doi:10.1371/journal.pone.0087851.
- [30] H. Falke, A. Chaikuad, A. Becker, N. Loačec, O. Lozach, S. Abu Jhaisha, W. Becker, P.G. Jones, L. Preu, K. Baumann, S. Knapp, L. Meijer, C. Kunick, 10-iodo-1H-indolo[3,2-c]quinoline-6-carboxylic acids are selective inhibitors of DYRK1A, *J. Med. Chem.* 58 (2015) 3131–3143. doi:10.1021/jm501994d.
- [31] T.T. Wager, R.Y. Chandrasekaran, X. Hou, M.D. Troutman, P.R. Verhoest, A. Villalobos, Y. Will, Defining desirable central nervous system drug space through the alignment of molecular properties, in vitro ADME, and safety attributes, *ACS Chem. Neurosci.* 1 (2010) 420–434. doi:10.1021/cn100007x.
- [32] S. Udenfriend, B. Witkop, B.G. Redfield, H. Weissbach, Studies with reversible inhibitors of monoamine oxidase: Harmaline and related compounds, *Biochem. Pharmacol.* 1 (1958) 160–165. doi:10.1016/0006-2952(58)90025-X.
- [33] G.D. Cuny, N.P. Ulyanova, D. Patnaik, J.-F. Liu, X. Lin, K. Auerbach, S.S. Ray, J. Xian, M.A. Glicksman, R.L. Stein, J.M. Higgins, Structure-activity relationship study of beta-carboline derivatives as haspin kinase inhibitors, *Bioorg. Med. Chem. Lett.* 22 (2012) 2015–2019. doi:10.1016/j.bmcl.2012.01.028.
- [34] R. Prudent, V. Moucadel, M. López-Ramos, S. Aci, B. Laudet, L. Mouawad, C. Barette, J. Einhorn, C. Einhorn, J.N. Denis, G. Bisson, F. Schmidt, S. Roy, L. Lafanechere, J.C. Florent, C. Cochet, Expanding the chemical diversity of CK2 inhibitors, *Mol. Cell. Biochem.* 316 (2008) 71–85. doi:10.1007/s11010-008-9828-z.
- [35] A.G. Golub, V.G. Bdzholia, N. V Briukhovetska, A.O. Balanda, O.P. Kukhareno, I.M. Kotev, O.V. Ostrynska, S.M. Yarmoluk, Synthesis and biological evaluation of substituted (thieno[2,3-d]pyrimidin-4-ylthio)carboxylic acids as inhibitors of human protein kinase CK2, *Eur. J. Med. Chem.* 46 (2011) 870–876. doi:10.1016/j.ejmech.2010.12.025.
- [36] L.A. Dakin, M.H. Block, H. Chen, E. Code, J.E. Dowling, X. Feng, A.D. Ferguson, I. Green, A.W. Hird, T. Howard, E.K. Keeton, M.L. Lamb, P.D. Lyne, H. Pollard, J. Read, A.J. Wu, T. Zhang, X. Zheng, Discovery of novel benzylidene-1,3-thiazolidine-2,4-diones as potent and selective inhibitors of the PIM-1, PIM-2, and PIM-3 protein kinases, *Bioorg. Med. Chem. Lett.* 22 (2012) 4599–4604. doi:10.1016/j.bmcl.2012.05.098.
- [37] H. de Koning, W.N. Speckamp, Succinimide, in: *Encycl. Reagents Org. Synth.*, John Wiley & Sons, Ltd, 2001. doi:10.1002/047084289X.rs126.
- [38] G.G. Alfonso, J.L.G. Ariza, Derivatives of rhodanine as spectrophotometric analytical reagents, *Microchem. J.* 26 (1981) 574–585. doi:10.1016/0026-265X(81)90144-2.
- [39] T. Mendgen, C. Steuer, C.D. Klein, Privileged scaffolds or promiscuous binders: a comparative study on rhodanines and related heterocycles in medicinal chemistry, *J. Med. Chem.* 55 (2012) 743–753. doi:10.1021/jm201243p.
- [40] M.A. Pagano, L. Cesaro, F. Meggio, L.A. Pinna, Protein kinase CK2: a newcomer in the “druggable kinome”, *Biochem. Soc. Trans.* 34 (2006) 1303–1306. doi:10.1042/BST0341303.
- [41] D.I. Perez, C. Gil, A. Martinez, Protein kinases CK1 and CK2 as new targets for neurodegenerative diseases, *Med. Res. Rev.* 31 (2011) 924–954. doi:10.1002/med.20207.
- [42] S. Côté, P.-H. Carmichael, R. Verreault, J. Lindsay, J. Lefebvre, D. Laurin, Nonsteroidal anti-inflammatory drug use and the risk of cognitive impairment and Alzheimer’s disease, *Alzheimers. Dement.* 8 (2012) 219–226. doi:10.1016/j.jalz.2011.03.012.
- [43] M. Camps, T. Rückle, H. Ji, V. Ardissonne, F. Rintelen, J. Shaw, C. Ferrandi, C. Chabert, C. Gillieron, B. Françon, T. Martin, D. Gretener, D. Perrin, D. Leroy, P.A. Vitte, E. Hirsch, M.P. Wymann, R. Cirillo, M.K. Schwarz, C. Rommel, Blockade of PI3Kgamma suppresses joint inflammation and damage in mouse models of rheumatoid arthritis, *Nat. Med.* 11 (2005) 936–943. doi:10.1038/nm1284.
- [44] X. Peng, X. Wu, L. Chen, Z. Wang, X. Hu, L. Song, C.M. He, Y.F. Luo, Z.Z. Chen, K. Jin, H.G. Lin, X.L. Li, Y.S. Wang, Y.Q. Wei, Inhibition of phosphoinositide 3-kinase ameliorates dextran sodium sulfate-induced colitis in mice, *J. Pharmacol. Exp. Ther.* 332 (2010) 46–56. doi:10.1124/jpet.109.153494.
- [45] Z. Wang, X. Wu, L. Song, Y. Wang, X. Hu, Y.F. Luo, Z.Z. Chen, J. Ke, X.D. Peng, C.M. He, W. Zhang, L.J. Chen, Y.Q. Wei, Phosphoinositide 3-kinase gamma inhibitor ameliorates concanavalin A-induced hepatic injury in mice, *Biochem. Biophys. Res. Commun.* 386 (2009) 569–574. doi:10.1016/j.bbrc.2009.06.060.
- [46] X. Wei, J. Han, Z. Chen, B. Qi, G. Wang, Y.H. Ma, H. Zheng, Y.F. Luo, Y.Q. Wei, L.J. Chen, A phosphoinositide 3-kinase-gamma inhibitor, AS605240 prevents bleomycin-induced pulmonary fibrosis in rats, *Biochem. Biophys. Res. Commun.* 397 (2010) 311–317. doi:10.1016/j.bbrc.2010.05.109.
- [47] V. Spitzenberg, C. König, S. Ulm, R. Marone, L. Röpke, J.P. Müller, M. Grün, R. Bauer, I. Rubio, M.P. Wymann, A. Voigt, R. Wetzker, Targeting PI3K in neuroblastoma, *J. Cancer Res. Clin. Oncol.* 136 (2010) 1881–1890. doi:10.1007/s00432-010-0847-2.
- [48] M. Mariano, C. Schmitt, P. Miralinaghi, M. Catto, R.W. Hartmann, A. Carotti, M. Engel, First Selective Dual Inhibitors of Tau Phosphorylation and Beta-Amyloid Aggregation, Two Major Pathogenic Mechanisms in Alzheimer’s Disease, *ACS Chem. Neurosci.* 5 (2014) 1198–1202. doi:10.1021/cn5001815.
- [49] E. Arsovska, J. Trontelj, N. Zidar, T. Tomašić, L.P. Mašić, D. Kikelj, J. Plavec, A. Zega, Evaluation of Michael-type acceptor reactivity of 5-benzylidenebarbiturates, 5-benzylidenerhodanines, and related heterocycles using NMR, *Acta Chim. Slov.* 61 (2014) 637–644.
- [50] G. Caillé, L.M. Dubé, Y. Théorêt, F. Varin, N. Mousseau, I.J. McGilveray, Stability study of diltiazem and two of its metabolites

- [51] O.D. Ratnoff, I.H. Lepow, Some properties of an esterase derived from preparations of the first component of complement, *J. Exp. Med.* 106 (1957) 327–343.
- [52] M.A. Khanfar, R.A. Hill, A. Kaddoumi, K.A. El Sayed, Discovery of novel GSK-3 β inhibitors with potent in vitro and in vivo activities and excellent brain permeability using combined ligand- and structure-based virtual screening, *J. Med. Chem.* 53 (2010) 8534–8545. doi:10.1021/jm100941j.
- [53] G.F. Passos, C.P. Figueiredo, R.D.S. Prediger, K.A.B.S. Silva, J.M. Siqueira, F.S. Duarte, P.C. Leal, R. Medeiros, J.B. Calixto, Involvement of phosphoinositide 3-kinase gamma in the neuro-inflammatory response and cognitive impairments induced by beta-amyloid 1-40 peptide in mice, *Brain. Behav. Immun.* 24 (2010) 493–501. doi:10.1016/j.bbi.2009.12.003.
- [54] D. Frost, B. Meechoovet, T. Wang, S. Gately, M. Giorgetti, I. Shcherbakova, T. Dunckley, β -carboline compounds, including harmine, inhibit DYRK1A and tau phosphorylation at multiple Alzheimer's disease-related sites, *PLoS One.* 6 (2011) e19264. doi:10.1371/journal.pone.0019264.

Acknowledgments

The authors thank Mrs. Nadja Weber and Dr. Christian Schmitt for performing some kinase inhibition assays. The financial support by the Deutsche Forschungsgemeinschaft (DFG) to M.E. (grant EN 381/2-3) is also greatly acknowledged.

Supplementary Material

Supplementary data associated with this article can be found in the online version.

These data include general synthetic methods, further compound syntheses and analytical data, Tables S1–S3 and the MTT assay method.

Figure 1. 2D structures of harmine, INDY and Leucettamine B.

Figure 2. Superimposition of harmine (green), INDY (cyan) and Leucettine L41 (magenta) cocrystallized with Dyrk1A (PDB codes 3ANR, 3ANQ and 4AZE, respectively). All ligands are bound in the ATP-binding cleft *via* two H-bonds, formed with Leu241-NH at the hinge region and Lys188 (indicated by the grey dashed lines). The measured ranges of the N–O distances are given in Å. Additional contacts comprise van der Waals-interactions with the side chains of Ala186, Val173 and Leu294, which mainly involve the left aromatic rings.

Figure 3. Inhibition of Dyrk1A-catalyzed tau-Thr212 phosphorylation in stably transfected HEK293 cells. The test compounds, DMSO or the reference inhibitor harmine [54] were added to the cell medium and the Dyrk1A expression induced as described. After immunoblotting of the total cell proteins, the level of phospho-tau-Thr212 was detected using a phosphospecific antibody. To normalize the signals, total recombinant GFP-tau protein was quantified on the same blot using an anti-GFP antibody (fluorescence image converted to grey scales). Initial screenings were performed at 1 µM compound concentrations (lower panel; one representative experiment out of two is shown). ^aIC₅₀ values were determined after cell treatment with different concentrations in triplicates, referring to the signal derived from DMSO-treated cells as 100%. Values represent averages from at least two independent determinations (±S.D.); AS, AS605240.

Table 1. Inhibitory activity of α -benzylidene- γ -butyrolactone derivatives against Dyrk1A and selectivity profiling against a panel of selected kinases.

^aS.D.≤18%, [ATP]=100µM; D1A=Dyrk1A, D1B=Dyrk1B, D2=Dyrk2; Hrm=Harmine; n.i., no inhibition; n.d., not determined.

Table 2. Inhibitory activity of benzylidene thioxothiazolidinone-based derivatives against Dyrk1A and selectivity profiling against a panel of selected kinases.

^aS.D.≤18%, [ATP]=100µM; D1A=Dyrk1A, D1B=Dyrk1B, D2=Dyrk2, AS= AS605240; n.d., not determined; n.i., no inhibition.

Table 3. Extended selectivity profiling of **16** and **17**.

^a% inhibition at 1 µM; shown are mean values of two different measurements performed in duplicates (S.D. ≤ 2.5%); ^bIC₅₀s were only determined when the % inhibition at 1 µM was greater than 85%. Data were calculated based on mean values of duplicates that differed by less than 7%.

Table 4. Metabolic stability in rat plasma.

^amean values from two experiments, S.D.< 17%; ^bno degradation detected after 120 min

Systematic diversification of benzylidene heterocycles yields novel inhibitor scaffolds selective for Dyrk1A, Clk1 and CK2

Marica Mariano^a, Rolf W. Hartmann^{a,b} and Matthias Engel^{a,*}

^a Department of Pharmaceutical and Medicinal Chemistry, Saarland University, Saarbrücken, Germany.

^b Helmholtz Institute for Pharmaceutical Research Saarland (HIPS), Campus C2-3, D 66123 Saarbrücken, Germany

Highlights

- A new α -benzylidene- γ -butyrolactone scaffold was designed and systematically diversified
- Different scaffolds exhibiting selectivity for Dyrk1A, Clk1 and CK2 were identified, with IC_{50} s from the low micromolar to the nanomolar range
- Multi-targeted kinase inhibitors were also obtained, that co-inhibited the lipid kinases PI3K α/γ
- Compounds possessing different scaffolds inhibited tau phosphorylation in intact cells

* Corresponding author. E-mail: ma.engel@mx.uni-saarland.de; phone: +4968130270312.